Nanomechanics of order reconstruction in nematic liquid crystals

Fulvio Bisi and Epifanio G. Virga
Dipartimento di Matematica, Istituto Nazionale di Fisica della Materia, Università di Pavia, via Ferrata 1, 27100 Pavia, Italy

Georges E. Durand
Laboratoire de Physique des Solides associé au CNRS (LA2), Université Paris Sud, F-91405 Orsay Cedex, France
(Received 16 April 2004; published 29 October 2004)

We employ a continuum model to compute both torque and force transmitted through a thin twist cell filled with a nematic liquid crystal and bounded by flat plates with anchorings at right angles. The transmitted torque vanishes at the order reconstruction threshold when the cell thickness is comparable with the biaxial coherence length. At the same point, the force diagram exhibits an angular point which disappears above a critical twist mismatch. Both torque and force diagrams against the cell's thickness fail to be monotonic when the total twist is near $\pi/2$.

DOI: 10.1103/PhysRevE.70.042701 PACS number(s): 61.30.Dk, 61.30.Pq

Ordering of nanostructures is an open question in phase transition physics and it has recently attracted considerable interest. In this respect, liquid crystals constitute one of the best model systems for both experiments and mathematical theories, especially in those situations where antagonistic surface constraints interfere with the order in the bulk. Recently, interesting experiments on nanoforces in nematic liquid crystals have been performed [1–4] to relate mechanical properties and local ordering. Similarly, bulk order transitions under strong external fields have been described where the spontaneous nematic order is first destroyed and then reconstructed [5]. *Order reconstruction* is what elsewhere in the literature is also called *eigenvalue exchange* [6,7], a terminology that refers to the representation of the nematic order in terms of a traceless, symmetric tensor $\mathbf{Q}$, which possesses two equal eigenvalues in the uniaxial states. Two uniaxial states can be transformed into one another either by rotating the eigenframe of $\mathbf{Q}$ or by letting one eigenvalue of $\mathbf{Q}$ grow at the expense of another, until a new uniaxial state, differently oriented, is reached through a wealth of biaxial states, where $\mathbf{Q}$ has different eigenvalues, while its eigenframe remains unchanged.

In this paper, we compute both torque and force in an ideal nanomachine where the surface ordering is prescribed on two antagonistic plates. In particular, we find that in the presence of order reconstruction the repulsive force between the plates is not monotonic, in contrast with the naive expectation that this force could only increase when the cell is squeezed.

We employ here the same mathematical model introduced in Ref. [8]. We consider a cell bounded by two parallel flat plates, $2d$ apart. The order tensor $\mathbf{Q}$ is assumed to be prescribed on both plates at its uniaxial bulk equilibrium value $\mathbf{Q}_0$ corresponding to the given temperature. On each boundary, the preferred axis of $\mathbf{Q}_0$ lies on the bounding plate. The angle between the two boundary orientations is φ_0, which ranges in $[0,\pi/2]$. Since the boundary conditions are uniform on both plates, we confine attention to a one-dimensional problem along the x axis orthogonal to the plates. The free energy F per unit area of the plates is given by

$$F[\mathbf{Q}]:=\int_{-d}^{+d}\left\{\frac{L}{2}|\mathbf{Q}'|^2+f_b(\mathbf{Q})\right\}dx, \tag{1}$$

where a prime denotes differentiation with respect to x and

$$f_b(\mathbf{Q}):=\frac{A}{2}\mathrm{tr}\,\mathbf{Q}^2-\frac{B}{3}\mathrm{tr}\,\mathbf{Q}^3+\frac{C}{4}(\mathrm{tr}\,\mathbf{Q}^2)^2. \tag{2}$$

Here we have employed a single elastic constant (L) in the gradient term. A, B, and C are the usual coefficients in the Landau–de Gennes bulk potential, of which $A=a(T-T^*)$ with $a>0$, where T is the current temperature and T^* is the supercooling temperature of the isotropic phase. The potential f_b is an expansion truncated at the fourth power, and so it should be accurate only close to the isotropic-nematic transition, but since it has also been used to fit experimental data in a wide range of temperatures below T^*, we reckon it is appropriate also there. Our definition of biaxial coherence length is [8,9]

$$\xi_b:=\sqrt{\frac{4LC}{B^2(1+\sqrt{1-\vartheta})}}, \tag{3}$$

where $\vartheta<1$ is the reduced temperature defined by

$$\vartheta:=\frac{T-T^*}{T^{**}-T^*}$$

and $T^{**}:=T^*+B^2/24aC$ is the superheating temperature of the nematic phase. In our model, the typical length is ξ_b; it lies in the range between a few nanometers and ten nanometers. Continuum theory has already been employed successfully both to describe pretransitional effects in thin films [10,11] and to explore the disclination core [12]: we pursue this line of thought and assume that continuum theory is also applicable at the ξ_b scale to describe mechanical properties.

Here we compute both the torque and the force exerted per unit area on the plates by the intervening liquid crystal as functions of the cell thickness $2d$. We achieve this by a variational argument: both torque and force will be related to conservation laws associated with the equilibrium equations for the free-energy functional F [8,13]. We first consider the variation of $\mathbf{Q}$ expressed by

$$\mathbf{Q}_\varepsilon := \mathbf{Q} + \varepsilon(\mathbf{WQ} - \mathbf{QW}) + o(\varepsilon), \tag{4}$$

where $\mathbf{W}$ is a skew-symmetric tensor depending on x and such that $\mathbf{W}(\pm d)=\mathbf{0}$. $\mathbf{Q}_\varepsilon$ represents the same order as $\mathbf{Q}$, but in a frame locally twisted by $\mathbf{W}$. Requiring F to be stationary at $\varepsilon=0$ along the trajectory described by Eq. (4), we arrive at

$$\delta F = L\int_{-d}^{+d} \mathbf{W}' \cdot (\mathbf{Q}'\mathbf{Q} - \mathbf{Q}\mathbf{Q}')dx = 0, \tag{5}$$

whence, by integration by parts and use of the boundary conditions on $\mathbf{W}$, we obtain that

$$\delta F = -L\int_{-d}^{+d} \mathbf{W} \cdot (\mathbf{Q}'\mathbf{Q} - \mathbf{Q}\mathbf{Q}')'dx = 0 \quad \text{for all } \mathbf{W}.$$

This condition requires the tensor

$$\mathbf{M} := -L(\mathbf{Q}'\mathbf{Q} - \mathbf{Q}\mathbf{Q}')$$

to be uniform throughout the cell. We now compute the free-energy difference, still denoted by δF, between two equilibrium states of the cell that differ by a small change $\delta\varphi_0$ in the total twist. It follows from Eq. (5) and the uniformity of $\mathbf{M}$ that

$$\delta F = -\boldsymbol{m} \cdot \delta\varphi_0 \boldsymbol{e}_x,$$

where $\boldsymbol{m}$ is the axial vector associated with $2\mathbf{M}$, which can thus be interpreted as the torque transmitted per unit area from one plate to the other. Similarly, we consider the following domain variation for $\mathbf{Q}$. We define $x_\varepsilon := x+\varepsilon u$, where u is an internal one-dimensional displacement that depends on x and obeys $u(\pm d)=0$, and we set

$$\mathbf{Q}_\varepsilon(x_\varepsilon) := \mathbf{Q}(x). \tag{6}$$

Requiring F to be stationary at $\varepsilon=0$ along the trajectory defined by Eq. (6), we arrive at

$$\delta F = \int_{-d}^{+d} \left\{ f_b(\mathbf{Q}) - \frac{L}{2}|\mathbf{Q}'|^2 \right\} u'dx = 0, \tag{7}$$

whence, by integration by parts and use of the boundary conditions on u, we obtain that

$$\delta F = -\int_{-d}^{+d} \left\{ f_b(\mathbf{Q}) - \frac{L}{2}|\mathbf{Q}'|^2 \right\}' u dx = 0 \quad \text{for all } u.$$

This condition requires

$$f := -\left(f_b(\mathbf{Q}) - \frac{L}{2}|\mathbf{Q}'|^2 \right) \tag{8}$$

to be uniform throughout the cell. We now compute the free-energy difference δF between two equilibrium states of the cell that differ only by a small displacement δd of the plates. It follows from Eq. (7) and the uniformity of f that

$$\delta F = -f\delta d.$$

Thus f can be interpreted as the force transmitted per unit area from one plate to the other. The symmetry of the boundary conditions suggests to consider equilibrium solutions $\mathbf{Q}$ for F that have everywhere $\boldsymbol{e}_x$ as an eigenvector. Under this assumption, $\boldsymbol{m}=m\boldsymbol{e}_x$.

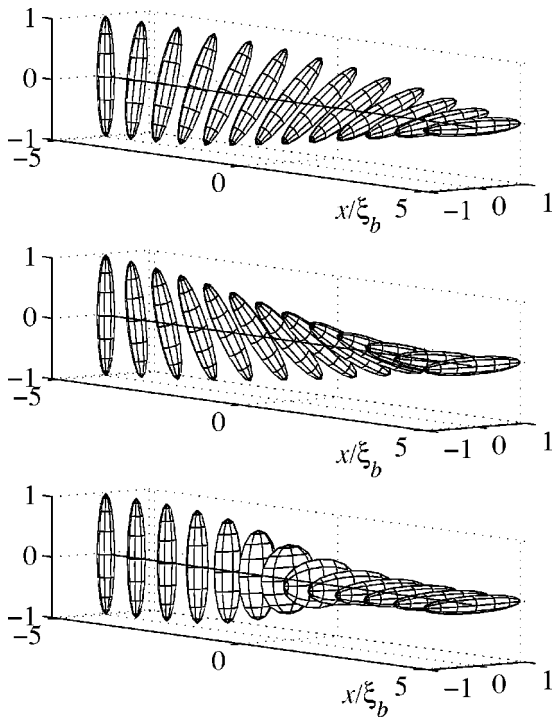

FIG. 1. Order-tensor ellipsoids against position across the cell, in units of the biaxial coherence length ξ_b, for three basic solutions: opposite twists (top and middle), order-reconstruction (bottom). Ellipsoids are oriented along the eigenframe of the order tensor $\mathbf{Q}$ at each point; their semiaxes are the eigenvalues of $\mathbf{Q}$ appropriately augmented and scaled to the largest eigenvalue at the boundary. Parameters: twist angle $\varphi_0=\pi/2$, reduced temperature $\vartheta=-8$, dimensionless cell half width $d/\xi_b=5$.

It was already shown [8] that, for $\varphi_0=\pi/2$, a texture bifurcation appears in the twist cell for $d=d_c\approx 2.5\xi_b$. For $d<d_c$, there is only one equilibrium texture that bridges the boundary conditions through order reconstruction: the eigenframe of $\mathbf{Q}$ remains unchanged throughout the cell, while the transverse eigenvalues in the (x,y) plane are exchanged. For $d>d_c$, the reconstruction texture becomes unstable and two stable symmetric textures emerge from it, corresponding to opposite twists of the transverse eigenvectors of $\mathbf{Q}$. Figure 1 illustrates all three types of equilibrium textures for $\varphi_0=\pi/2$.

The classical pitchfork picture now outlined is unfolded as φ_0 departs from $\pi/2$. The texture with minimum twist is stable for all values of d; the texture with maximum twist is locally stable above a critical value $d_c'>d_c$ of d that increases as φ_0 decreases. As in Ref. [8], we computed numerically both m and f with the aid of AUTO 2000 [14]; the mathematical details of this work will be published elsewhere [13]. In Fig. 2, m is plotted against d for $\vartheta=-8$ and $0.35\pi \leqslant \varphi_0 \leqslant \pi/2$ in the units $m_0=B^3L^{1/2}/C^{5/2}$. For the typical values of 5CB [15], namely, $B=7.2$ MJ m^{-3}, $L=9.1$ pN, and $C=8.8$ MJ m^{-3}, $m_0\approx 5$ mJ m^{-2}, and $\xi_b\approx 1$ nm at the reduced temperature $\vartheta=-8$. This choice of ϑ, though realistic by all means, is somehow cabalistic, as it was shown in Ref. [8] that for $\vartheta=-8$ all equilibrium textures possess an order

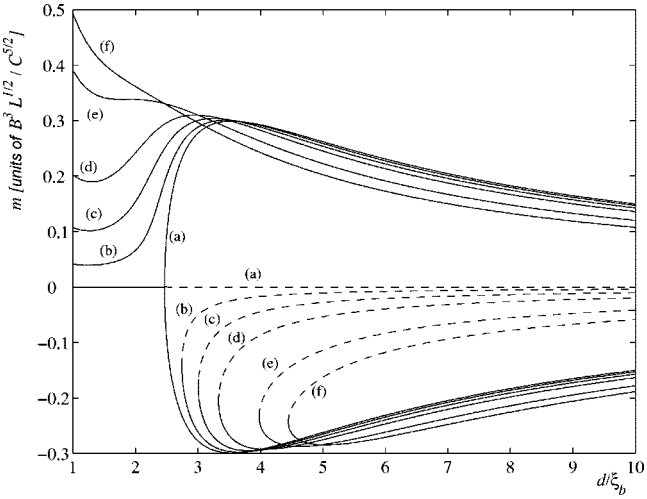

FIG. 2. The torque m transmitted per unit area from one plate to the other is plotted against the half thickness d of the cell scaled to the biaxial coherence length ξ_b in Eq. (3), for $\vartheta=-8$ and different values of the total twist angle: (a) $\varphi_0=\pi/2$, (b) $\varphi_0=0.49\pi$, (c) $\varphi_0=0.474\pi$, (d) $\varphi_0=0.45\pi$, (e) $\varphi_0=0.394\pi$, and (f) $\varphi_0=0.35\pi$. For each value of φ_0, stable branches are represented by solid lines, while unstable branches are represented by dashed lines. For $\varphi_0=\pi/2$, the graphs corresponding to the two symmetric twist textures merge with the reconstruction straight line bearing no torque at $d=d_c\approx 2.5\xi_b$. For $\varphi_0<\pi/2$, the upper stable branches (with $m>0$) correspond to the least twisted textures, which meet with the unstable reconstruction branch at different values d_c' of d, depending on φ_0. Here m is scaled to $m_0=B^3L^{1/2}/C^{5/2}\approx 5$ mJ m^{-2} for 5CB, and $\xi_b\approx 1$ nm for the same material.

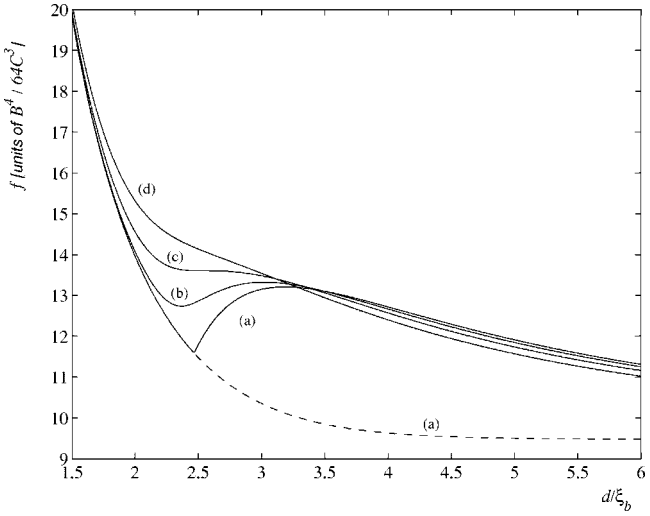

FIG. 3. The force f transmitted per unit area from one plate to the other is plotted against the half thickness d of the cell scaled to the biaxial coherence length ξ_b, for $\vartheta=-8$ and different values of the total twist angle: (a) $\varphi_0=\pi/2$, (b) $\varphi_0=0.49\pi$, (c) $\varphi_0=\varphi_c^*\approx 0.474\pi$, (d) $\varphi_0=0.45\pi$. For $\varphi_0=\pi/2$, the dashed branch corresponds to the unstable reconstruction texture, which becomes stable at $d=d_c\approx 2.5\xi_b$, where it meets the stable branch corresponding to the two symmetric twists. For $\varphi_0<\pi/2$, only the stable branches corresponding to the least twisted textures are plotted: they are the counterparts of the upper stable branches in the torque diagrams of Fig. 2. Here f is scaled to $f_0=B^4/64C^3\approx 60$ mPa for 5CB, and $\xi_b\approx 1$ nm.

tensor $\mathbf{Q}$ with an eigenvalue constant throughout the cell.

For $\varphi_0=\pi/2$, the graph of m gives a direct representation of the texture bifurcation. When $\varphi_0<\pi/2$, the stable branch of the torque diagram diverges like $1/d$ as d decreases; it exhibits a minimum for $d=d_m$ and a maximum for $d=d_M>d_m$, until φ_0 reaches the critical value $\varphi_c\approx 0.394\pi$, at which minimum and maximum merge in an inflection point. For $\varphi_0<\varphi_c$, the stable branch of the torque diagram is monotonic and for all values of φ_0 it decays to zero like $1/d$ as $d\gg\xi_b$. In principle, on each plate the prescribed uniaxial orientation of $\mathbf{Q}_0$ can be controlled by a suitable surface treatment: the angle φ_0 is a macroscopically controllable quantity. Measuring m as a function of d for a given φ_0 should reproduce the unfolded bifurcation diagram in Fig. 2, thus leading to a direct mechanical measurement of ξ_b. In particular, for $\varphi_c<\varphi_0<\pi/2$ a snapping instability should be met upon decreasing d through the critical value d_M, since there the equilibrium torque would decrease. However, in practice, nanotorque machines are not yet developed. There are, on the other hand, established nanoforce machines [16,17]; this urges us to seek how the texture bifurcation is also reflected onto the force diagram. In Fig. 3, this diagram is plotted for $0.45\pi\leqslant\varphi_0\leqslant\pi/2$ in the units $f_0=B^4/64C^3$.

In accordance with Eq. (8), for large values of d the force f tends to $-f_m$, where f_m is the minimum of f_b, independent of φ_0; f decays to $-f_m$ as $1/d^2$ decays to zero. For $\varphi_0=\pi/2$, upon reducing d, the force exerted by both twist textures increases as long as $d>d_M^*$ and then decreases until it meets the force exerted by the reconstruction texture at $d=d_c$. Upon further reducing d below d_c, the reconstruction force keeps increasing and diverges like $1/d^2$. The slope of the graph of f against d is discontinuous at $d=d_c$, where m vanishes. For $\varphi_0<\pi/2$, the force diagram is unfolded: the angular point at d_c evolves into a regular minimum at d_m^*, which survives until φ_0 reaches the critical value $\varphi_c^*\approx 0.474\pi$. Here both d_M^* and d_m^*, which also depend on φ_0, are generally different from d_M and d_m, respectively. In particular, for our choice of parameters, $d_M^*<d_M$ and $d_m^*>d_m$. For $\varphi_0<\varphi_c^*$, f becomes strictly monotonic. For 5CB, $f_0\approx 60$ mPa, and so, taking 10^{-8} N as the typical sensitivity of a force machine [17], we estimate that the nanoscopic force f would be measurable for plates of area ℓ^2, provided that $\ell>400$ μm. This appears to be a reasonable size. We thus believe that the mechanical signature of the bifurcation related to order reconstruction could actually be observed. Moreover, as for the torque diagrams, the lack of monotonicity in the force diagrams would imply that a snapping instability is expected to be experienced by the machine at d_M^*.

In Fig. 4, the total free energy F stored in the cell per unit area of the bounding plates is plotted for the same values of φ_0 in the force diagrams of Fig. 3. In all these graphs, F diverges like $1/d$ when $d\ll\xi_b$ and behaves like $f_m d$ for $d\gg\xi_b$. F is a monotonic function of d for all φ_0. Since, on the contrary, f is not monotonic for $\pi/2\leqslant\varphi_0\leqslant\varphi_c^*$, much care should be taken in employing approximations that would derive f by simply rescaling F, as is the case for Derjaguin's approximation [18] often invoked also to estimate the force

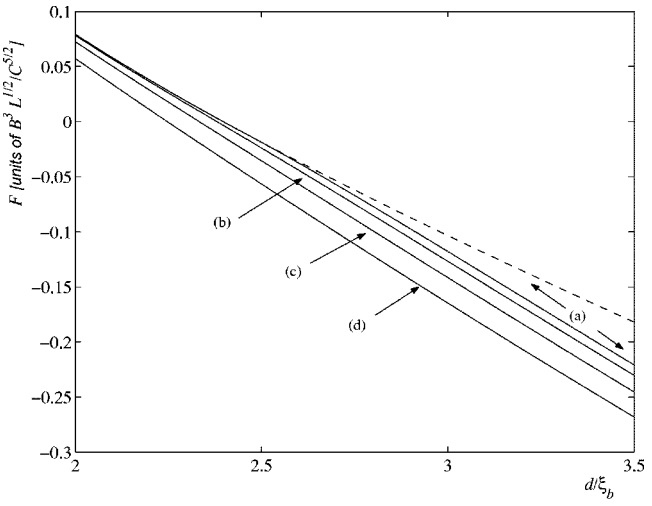

FIG. 4. The total free energy F per unit area of the cell's plates is plotted against the half thickness d of the cell for $\vartheta=-8$ and the same vales of φ_0 as in Fig. 3: (a) $\varphi_0=\pi/2$, (b) $\varphi_0=0.49\pi$, (c) $\varphi_0=\varphi_c^*\approx 0.474\pi$, (d) $\varphi_0=0.45\pi$. The dashed curve corresponds to the unstable reconstruction texture. Here F is scaled to m_0, the same units employed in Fig. 2 for the torque m.

exerted on curved walls by an intervening liquid crystal [1–3,19,20]. Our computations show that such an approximation could miss fine details of the force diagram, such as its lack of monotonicity and the instabilities associated with this.

To conclude, we computed both the nanotorque m and the nanoforce f transmitted between two parallel plates $2d$ apart, confining a nematic liquid crystal in a φ_0-twist cell with infinitely strong anchoring. Measuring $m(d)$ for φ_0 close to $\pi/2$ would provide the most direct evaluation of the biaxial coherence length ξ_b. It may be more practical to employ a nanoforce machine where the order reconstruction appears as an angular point in the diagram of $f(d)$. For $\varphi_0=\pi/2$, both the torque and the force diagrams are not monotonic. We predicted the existence of two critical twist angles φ_c and $\varphi_c^*>\varphi_c$, below which the torque and the force diagrams, respectively, become strictly monotonic. Clearly, our theory gives only the continuum contribution to nanoforces. A more accurate description should also account for other forces, such as van der Waals's and Casimir's, which are likely to affect the divergence of f predicted here for $d\ll\xi_b$. In principle, these forces should also depend on the underlying liquid crystal texture. They will form the object of further studies. Similarly, the oscillating structural forces ascribed to the positional ordering of the molecules on the bounding plates [19] fall outside the scope of our analysis. A closer glance at the medium-range structural forces of liquid crystals, in the terminology of Ref. [19], has shown that they also fail to be monotonic, and this makes them less distinguishable from the short-range ones.

The possibility of using flat surfaces in nanoforce machines could be questioned, but previous experiments have shown that they are indeed possible [21], though they need to be improved to explore nanothicknesses. The assumption on infinite anchoring made here could also be questioned. Such an assumption seems, however, to be compatible with nanoscale observations of single nematic molecular layers on cleaved monocrystal surfaces [22–25].

We hope that mechanical measurements will foster a better understanding of nematic liquid crystals at the nanoscale.

[1] P. Richetti, L. Moreau, P. Barois, and P. Kékicheff, Phys. Rev. E **54**, 1749 (1996).
[2] K. Kočevar, R. Blinc, and I. Muševic, Phys. Rev. E **62**, R3055 (2000).
[3] K. Kočevar and I. Muševic, Phys. Rev. E **65**, 021703 (2002).
[4] B. Zappone, Ph.D. thesis, University of Bordeaux, France, 2004.
[5] R. Barberi, F. Ciuchi, G. E. Durand, M. Iovane, D. Sikharulidze, A. M. Sonnet, and E. G. Virga, Eur. Phys. J. E **13**, 61 (2004).
[6] N. Schopohl and T. J. Sluckin, Phys. Rev. Lett. **59**, 2582 (1987).
[7] P. Palffy-Muhoray, E. C. Gartland, and J. R. Kelly, Liq. Cryst. **16**, 713 (1994).
[8] F. Bisi, E. C. Gartland, R. Rosso, and E. G. Virga, Phys. Rev. E **68**, 021707 (2003).
[9] S. Kralj, E. G. Virga, and S. Žumer, Phys. Rev. E **60**, 1858 (1999).
[10] P. Sheng, Phys. Rev. Lett. **37**, 1059 (1976).
[11] K. Miyano, Phys. Rev. Lett. **43**, 51 (1979).
[12] N. Schopohl and T. J. Sluckin, Phys. Rev. Lett. **59**, 2582 (1987).
[13] F. Bisi and E. G. Virga (unpublished).
[14] See http://sourceforge.net/projects/auto2000
[15] H. Coles, Mol. Cryst. Liq. Cryst. Lett. **49**, 67 (1978).
[16] J. N. Israelaschvili and G. E. Adams, J. Chem. Soc., Faraday Trans. 1 **74**, 975 (1978).
[17] J. N. Israelaschvili, *Intermolecular and Surface Forces* (Academic, London, 1992).
[18] B. V. Derjaguin, Kolloid-Z. **69**, 155 (1934).
[19] R. G. Horn, J. N. Israelaschvili, and E. Perez, J. Phys. (France) **42**, 39 (1981).
[20] L. Moreau, P. Richetti, and P. Barois, Phys. Rev. Lett. **73**, 3556 (1994).
[21] M. Cagnon and G. Durand, Phys. Rev. Lett. **70**, 2742 (1993).
[22] J. S. Foster and J. E. Frommer, Nature (London) **333**, 542 (1988).
[23] J. K. Spong, H. M. Mizes, J. R. L. J. Lacomb, M. M. Dovek, J. E. Frommer, and J. S. Foster, Nature (London) **338**, 137 (1989).
[24] D. P. E. Smith, J. K. H. Hörber, G. Binnig, and N. Nejoh, Nature (London) **344**, 641 (1990).
[25] B. Jérôme, Rep. Prog. Phys. **54**, 391 (1991).